Published in Science Bulletin, 67, 2022, 1967-1970.
https://www.sciencedirect.com/science/article/pii/S2095927322003644

Winter accumulation drives the spatial variations in glacier mass balance in High Mountain Asia

Lei Huang [a,b], Regine Hock[c,d], Xin Li[e,f], Tobias Bolch[g], Kun Yang[h,f], Ning-lian Wang[i], Tan-dong Yao[e], Jian-min Zhou [a,b] , Chang-yong Dou [a,b] , Zhen Li [a,b]

[a]International Research Center of Big Data for Sustainable Development Goals, China.
[b]Aerospace Information Research Institute, Chinese Academy of Sciences, China.
[c]Department of Geosciences, Oslo University, Norway.
[d]Geophysical Institute, University of Alaska Fairbanks, USA.
[e]Institute of Tibet Plateau Research, Chinese Academy of Sciences, China.
[f]State Key Laboratory of Tibetan Plateau Earth System, Environment and Resources (TPESER), Institute of Tibetan Plateau Research, Chinese Academy of Sciences, Beijing 100101, China
[g]School of Geography & Sustainable Development, University of St Andrews, St Andrews, Scotland, UK.
[h]Department of Earth System Science, Tsinghua University, China
[i]Northwest University, China.

Email address: huanglei@radi.ac.cn (Lei Huang), lizhen@radi.ac.cn (Zhen Li).

High Mountain Asia has the largest volume of glacier ice outside the polar regions [1] and is considered the water tower of Asia [2]. These glaciers provide drinking and irrigation water for millions of people as well as ecosystems in and beyond the mountain ranges, and are especially important in drought-affected regions [3,4].

Recent estimates of region-wide glacier mass losses vary from -13 to -19 Gt. a^{-1} (-0.14 to -0.19 m w.e. a^{-1}) for various periods between 2000 and 2018 [5, 6]. The mass loss rates are on average less pronounced in High Mountain Asia than in other major glacierized regions on Earth such as Alaska [7] due to balanced or even positive mass budgets in some subregions. While glacier mass balances in Hengduan Shan were strongly negative during 2000 - 2018 (-0.64 ± 0.15 m w.e. a^{-1}), glaciers in Karakoram, Eastern Pamir and Western Kunlun were on average close to balance or exhibited even slightly positive mass budgets during this period [5, 6].

The unusually heterogeneous behaviour has been attributed to differences in glacier mass balance sensitivity to temperature change [8], enhanced westerlies and weakened Indian monsoons [9], increased winter precipitation [10], increased summer cloud cover and regional humidity [11]. Further factors explaining the differences are glacier morphology, surface albedo, debris cover and pro-glacial lakes. However, unambiguous attribution is still lacking [12].

Glaciers in High Mountain Asia can be divided into summer-accumulation type, which gain most mass from summer snow, winter-accumulation type, which gain most mass from winter snow [13], and transitional-accumulation type, which lacks a distinct accumulation season. Previous studies deriving the accumulation types have been based on climate models [11] or reanalysis products [8], which both face challenges due to insufficient spatial model resolution in steep terrain and scarcity of direct observations at high altitudes, in particular solid precipitation [14] to inform the models. Studies based on remote sensing and model-derived glacier mass balance and measured river discharge, show that precipitation at high altitude is strongly underestimated in many available gridded climate data sets [15].

Here we circumvent the need for climate data and propose a new index entirely based on glacier surface observations from space that characterizes the accumulation type. We calculate the extent of the firn (i.e. snow that has survived at least one summer) in winter and the zone with remaining (wet) summer snow at the end of the summer using Sentinel-1 C-band Synthetic Aperture Radar (SAR) and Landsat-8 Operational Land Imager (OLI) imagery and Google Earth Engine for 22 characteristic subregions including all glaciers in High Mountain Asia for each year between 2015 and 2018. All debris pixels within the RGI 6.0 outlines are excluded with Landsat images (see Methods in the Supplementary material, Fig. S1-S5).

In order to characterize each glacier's and subregion's dominant accumulation type we then compute a new glacier index defined by

$$I = \frac{A_{firn}}{A_{total}} - \frac{A_{wet\ snow}}{A_{total}}, \quad (1)$$

where A_{firn} is the area of the firn zone, $A_{wet\ snow}$ the area of the late summer wet snow zone and A_{total} the total glacier area. $\frac{A_{firn}}{A_{total}}$ and $\frac{A_{wet\ snow}}{A_{total}}$ are referred to as firn area ratio and wet snow area ratio, respectively. A_{firn} and $A_{wet\ snow}$ are normalized by A_{total} to account for different glacier sizes. The rationale behind the index I is illustrated in Fig. S1. The index can generally be expected to be positive for winter-accumulation-type glaciers since summer snow fall is rare and thus $A_{wet\ snow}$ smaller than A_{firn}. In contrast the index is more likely to be negative (larger wet summer snow area than firn area) for summer-accumulation-type glaciers due to frequent summer snow falls. The index is normalized relative to the firn-area ratio to account for glaciers in different mass balance states.

Fig. 1 shows the index derived from the firn and wet summer snow area extent for all glaciers in High Mountain Asia defined by RGI 6.0 as well as for each of the 22 subregions. The latter is computed from each subregion´s total firn and wet summer snow area. The index ranges from 0.73 to -0.71 for individual glaciers, while for the subregions it ranges from 0.24 in Western Kunlun Shan to -0.29 in Tanggula Shan (Fig. 2a). Glaciers and subregions with indices exceeding 0.05 are classified as winter-accumulation type while those with indices less than -0.05 are categorized as summer-accumulation type. The remaining glaciers and subregions where the index ranges between -0.05~0.05, are classified as transitional-accumulation type since the wet snow area and firn area ratio are of similar magnitude (Fig. 2b).

Winter-accumulation glacier types dominate in the western parts of High Mountain Asia including the Western and Eastern Pamir, Central Tien Shan, Western and Eastern Kunlun Shan, Altun Shan, Eastern Hindu Kush, Karakoram, Western Himalaya (Fig. 1), consistent with prevailing westerlies which are typically associated with higher winter snowfall. The southern part (Gangdise Mountains) and eastern part of the mountains of the Tibetan plateau (Tanggula Shan, Nyainqentanglha, Hengduan Shan and Eastern Tibetan Mountains) are classified as summer-accumulation type consistent with precipitation patterns influenced by the Indian and East Asian monsoon. Summer-accumulation types are also found at the northern edge of the region, such as the Northern/Western Tien Shan and Dzhungar Alatau, mainly due to frontal cyclonic activities which occur in early summer in this subregion and intrusions from cold and moist air masses from the north. Subregions classified as transitional are found scattered across High Mountain Asia, including the Eastern and Central Himalaya, Tibetan Interior Mountains, Qilian Shan and Pamir Alay.

Fig. 1. Results of satellite derived accumulation type for all glaciers in High Mountain Asia and for 22 subregions. Subregions correspond to the second-order Hindu Kush Himalayan Monitoring and Assessment Programme (HIMAP) regions [4]. Lighter to darker grey shades scale with increasing altitude. Arrows indicate main seasonal wind directions [8]. Numbers below each region name refer to mean specific mass rates (m w.e. a^{-1} for 2000-2018 [5]).

We show that the index is a powerful indicator of accumulation type and correlates well with the specific glacier mass balance (i.e. mass change per area unit). We use published regionally averaged mass-balance data for all 22 subregions from 2000 to 2018 which were derived from differencing high-resolution digital elevation models (DEM) covering 99% of all glacier area [5]. We find that the specific mass-balance rates differ clearly between accumulation types. The area-weighted mass-change rates for the winter-accumulation type, transitional-accumulation type, and summer-accumulation type glacier regions are -0.10 ± 0.06 m w.e. a^{-1}, -0.32 ± 0.10 m w.e. a^{-1}, -0.43 ± 0.12 m w.e. a^{-1}, respectively, for the period 2000-2018. Hence, winter-accumulation type glaciers have less negative balances than the other two types indicating that the seasonality of the accumulation covaries with the spatial variability in regional specific balance rates.

Each subregion's index used to distinguish between accumulation types correlates well with the corresponding specific mass-balance rates averaged over the period 2000 – 2018 (Fig. 2c). The greater the difference between firn and wet snow ratio, i.e. the stronger the indication that a subregion's glaciers are winter-accumulation type, the less negative the mass change. This correlation is driven largely by variations in firn area ratio (Fig. 2d) as there is no significant correlation with the wet snow area ratio (Fig. 2e). This result shows that the amount of winter snow accumulation plays a more important role in the mass balance of glaciers than the amount of summer snow.

Fig.2. Glacier index and its correlation with annual mass balance. a, Firn area ratio (FAR) and wet snow area ratio (WSAR) from 2015 to 2018 for 22 subregions. **b**, Difference between FAR and WSAR averaged over 2015 and 2018 used to discriminate accumulation type. Grey bars show ± 1 standard deviation. **c-e**. Correlation between annual specific mass balance and FAR-WSAR (**c**), FAR (**d**) and WSAR (**e**). Each dot with a number represents a subregion (Fig. 1). Vertical bars refer to mass-balance uncertainties [5] and horizontal bars denote the standard deviation of the annual FAR-WSAR values during 2015-2018. The linear regression model is displayed in dark grey with the 95% confidence intervals in light grey.

In several subregions our derived accumulation types using SAR data agree well with accumulation types estimated from seasonal precipitation using reanalysis and modelled gridded datasets [13, 14] (Table S1 and Fig. S6-8). This is especially the case for those subregions that are clearly under the prevailing influence of the westerlies (such as the Western Pamir, Eastern Hindu Kush and Karakoram) or the Indian or East Asian Summer monsoon (such as Gangdise Mountains, Nyainqentanglha or Tanggula Shan). However, discrepancies are found in some subregions including parts of Tien Shan, Eastern Pamir and Western Kunlun (Table S1). Most gridded precipitation data sets are typically informed by or bias corrected with in situ measurements at weather stations located in lower altitude valleys, and thus may not be fully representative of the high-altitude glacierised areas. For example, in Central Tien Shan, precipitation data collected at weather stations outside the glacier suggest summer-accumulation type. However, ablation stake observations and model-driven glacier-wide mass-balance reconstruction during 2003/04-2013/2014 indicate that the accumulation is higher in winter than in summer. In Northern/Western Tien Shan, which we classify as summer-accumulation type, records from weather stations at lower altitudes show that precipitation peaks in winter, while at the higher glacierised altitudes cyclonic activities, westerly winds and cold and moist air masses, together with convective precipitation cause a precipitation maximum in early summer; Also in valleys of Eastern Himalaya, precipitation mainly occurs in the summer monsoon season at altitudes below 2500 m a.s.l., while rain-gauge observations show that at 4000-4500 m a.s.l. precipitation peaks in both March-April and July-August (more details and references see Supplementary material). Hence, our satellite derived approach may provide more accurate estimates of the glacier accumulation type than those derived from currently available gridded or available weather station data sets.

We also note that the relation between our firn area- and wet snow area-based index and regional specific mass balance may vary in time as glaciers continue to retreat despite considering varying firn area extent in the calculation of the index (Equation 1). However, in our analysis this effect can be assumed small since we compute the index only over a few years of data. In this way we smooth out variations due to interannual variability but avoid significant impact of a mass-balance trend on the analysis. Thus we interpret any variations in the index as reflecting spatial variations in accumulation type. However, if the analysis was repeated after years of continued glacier retreat and mass loss, the current thresholds used to discriminate different accumulation types may need adjustment to avoid misclassification.

While previous research on the relationship between the seasonality of snow accumulation and glacier mass balance has relied on precipitation data to determine the accumulation type, here, for the first time, we use high-resolution regional-scale observations of the glaciers themselves.

Our results demonstrate that summer-accumulation type glaciers thin on average about four times faster than winter-accumulation type glaciers, indicating that our new index provides a powerful tool to support the characterization of glacier mass changes from space. Our large-scale SAR-based analysis of glacier surface properties can also help to enhance our understanding of the spatial variability of precipitation at high altitudes and improve projections of glacier mass change in High Mountain Asia.

Open Research

The datasets named Wet snow and Firn of glaciers in High Mountain Asia generated during the current study are available from the following website http://data.casearth.cn/en/sdo/detail/6184e3bd08415d692f1902d7.

References

[1] Millan R., Mouginot J., Rabatel, A. et al. Ice velocity and thickness of the world's glaciers. Nat Geosci 2022; 15: 124–129.

[2] Immerzeel W.W., Lutz A.F., Andrade M. et al. Importance and vulnerability of the world's water towers. Nature 2020; 577: 364-369.

[3] Pritchard, H. D. Asia's shrinking glaciers protect large populations from drought stress. Nature 2019; 569: 649-654.

[4] Su, B., Xiao, C., Chen, D. Mismatch between the population and meltwater changes creates opportunities and risks for global glacier-fed basins. Sci Bull 2022, 67:9-12.

[5] Bolch T, Shea J M, Liu S, et al. The Hindu Kush Himalaya Assessment Chapter 7: Status and Change of the Cryosphere in the Extended Hindu Kush Himalaya Region. Switzerland AG, Cham: Springer Nature; 2019.

[6] Shean D, Bhushan S, Montesano P, et al. A systematic, regional assessment of High Mountain Asia glacier mass balance. Front in Earth Sci 2020; 7(363). doi: 10.3389/feart.2019.00363.

[7] Hugonnet R, McNabb R, Berthier E, et al. Accelerated global glacier mass loss in the early twenty-first century. Nature 2021; 592: 726–731.

[8] Sakai A, Fujita K. Contrasting glacier responses to recent climate change in high mountain Asia. Sci Rep 2017; 7: 13717.

[9] Yao T, Thompson L, Yang W, et al. Different glacier status with atmospheric circulations in Tibetan Plateau and surroundings. Nat Clim Change 2012; 2: 663-667.

[10] Bashir F, Zeng X, Gupta H, Hazenberg P. A hydrometeorological perspective on the Karakoram anomaly using unique valley-based synoptic weather observations. Geophys Res Lett 2014; 44: 10470-10478.

[11] Kapnick S, Delworth T, Ashfaq M, et al. Snowfall less sensitive to warming in Karakoram than in Himalayas due to a unique seasonal cycle. Nat Geosci 2014; 7:834-840.

[12] Farinotti D, Immerzeel WW, de Kok, RJ, et al. Manifestations and mechanisms of the Karakoram glacier Anomaly. Nat Geosci 2020; 13: 8-16.

[13] Maussion F, Scherer D, Mölg T, et al. Precipitation seasonality and variability over the Tibetan Plateau as Resolved by the High Asia reanalysis. J Clim 2014; 27: 1910-1927.

[14] Sakai A, Nuimura T, Fujita K, et al. Climate regime of Asian glaciers revealed by GAMDAM glacier inventory. Cryosphere 2015; **9**: 865-880.

[15] Immerzeel WW, Wanders N, Lutz AF, et al. Reconciling high-altitude precipitation in the upper Indus basin with glacier mass balances and runoff. Hydrol Earth Syst Sci 2015; 19: 4673–4687.

Acknowledgements

This work is supported by the National Key Research and Development Program of China [Grant No. 2018YFA0605403], the National Science Foundation of China [41971393], the Strategic Priority Research Program of Chinese Academy of Sciences [Grant No. XDA20100300].

Author contributions

Lei Huang and Zhen Li designed and led the study, and developed the SAR-based method. Lei Huang prepared the data sets and performed most calculations. He designed the figures and developed the analyses, discussion and interpretation with substantial input from Regine Hock. Lei Huang and Regine Hock, with input from Tobias Bolch, wrote the paper. Xin Li, Ninglian Wang, and Tandong Yao contributed to the interpretation of the SAR results. Tobias Bolch. contributed to the interpretation of the accumulation types, the development of the gridded climate data analysis and its writing. Kun Yang analysed the HAR v2 data made the corresponding figures. Jianmin Zhou and Changyong Dou contributed to programming and data processing to extract snow and firn zones.

Competing interests

The authors declare no competing interests.

Figures

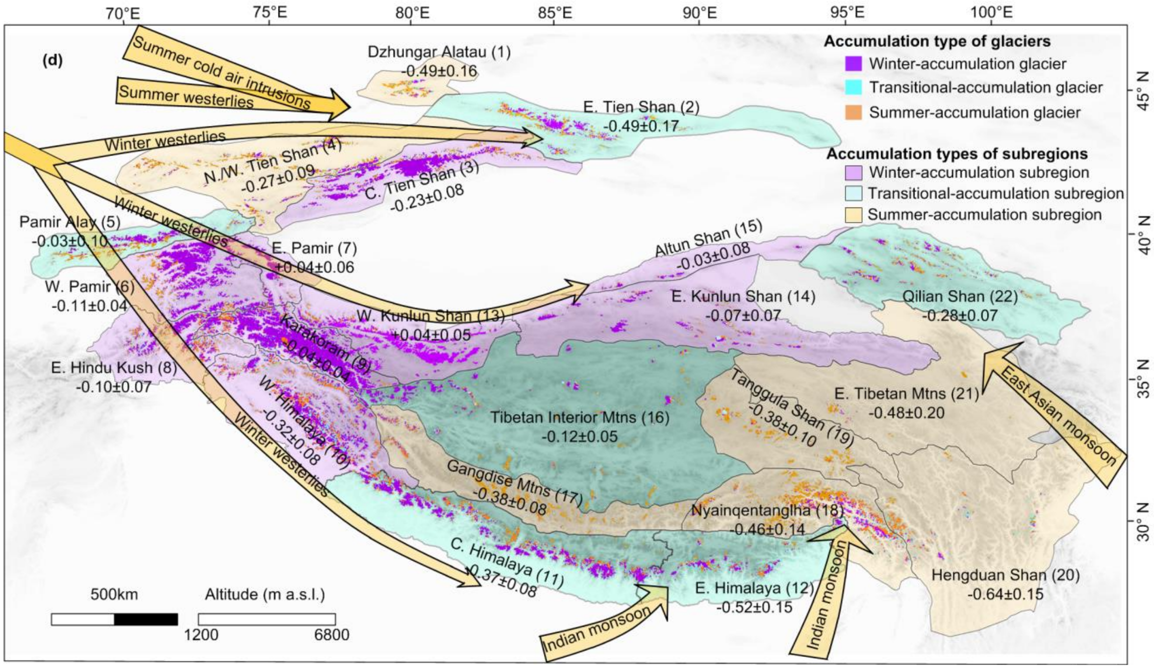

Fig. 1. Results of satellite derived accumulation type for all glaciers in High Mountain Asia and for 22 subregions. Subregions correspond to the second-order Hindu Kush Himalayan Monitoring and Assessment Programme (HIMAP) regions [4]. Lighter to darker grey shades scale with increasing altitude. The arrows indicate main seasonal wind directions [8]. The numbers below each region name refer to mean specific mass rates (m w.e. a^{-1} for 2000-2018 [5]).

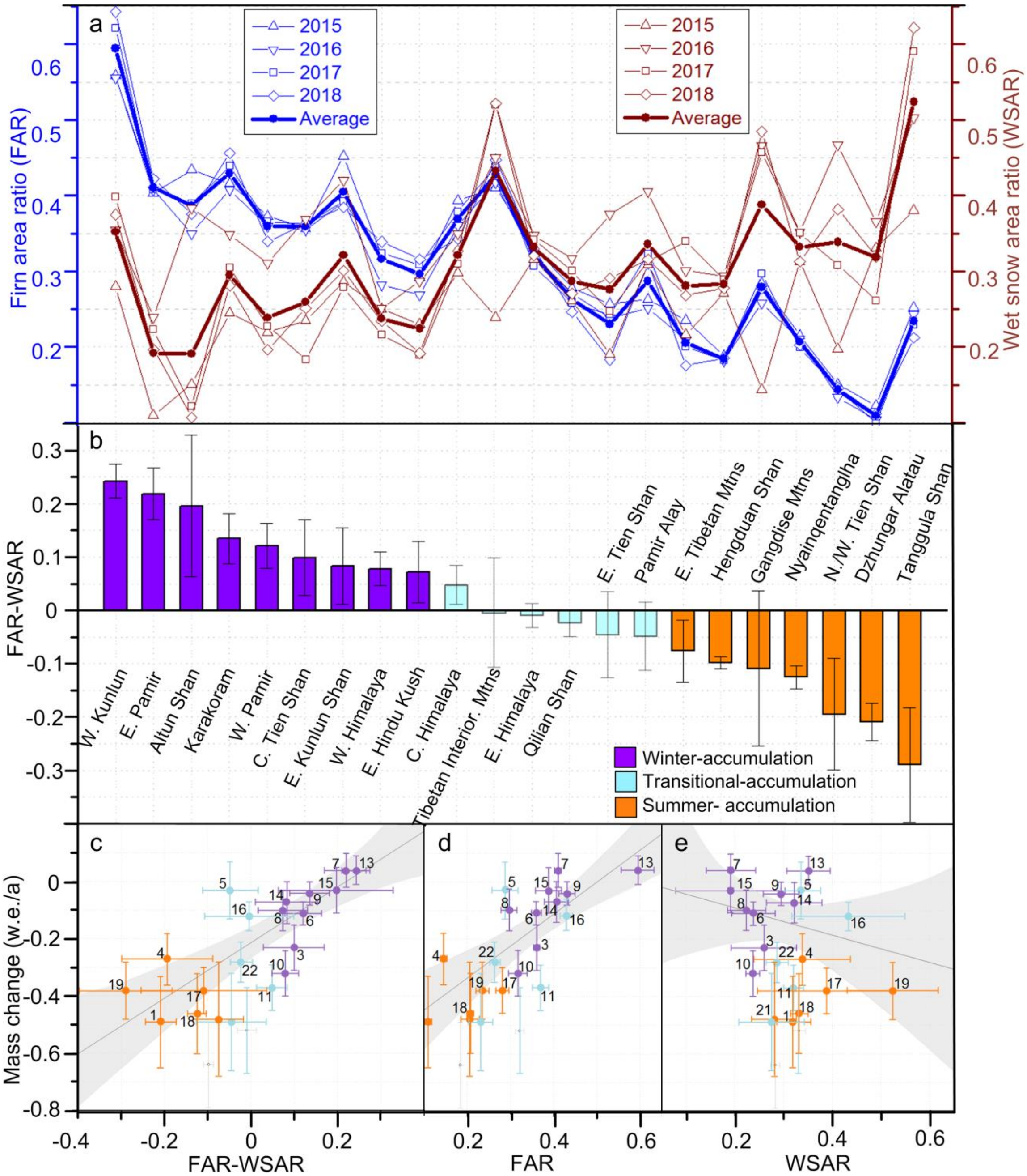

Fig.2. Glacier index and its correlation with annual mass balance. a, Firn area ratio (FAR) and wet snow area ratio (WSAR) from 2015 to 2018 for 22 subregions. **b**, Difference between FAR and WSAR averaged over 2015 and 2018 used to discriminate accumulation type. Grey bars show ± 1 standard deviation. **c-e**. Correlation between annual specific mass balance and FAR-WSAR (**c**), FAR (**d**) and WSAR (**e**). Each dot with a number represents a subregion (Fig. 1). Vertical bars refer to mass-balance uncertainties [5] and horizontal bars denote the standard deviation of the annual FAR-WSAR values during 2015-2018. The linear regression model is displayed in dark grey with the 95% confidence intervals in light grey.